ISA Transactions 53 (2014) 415–422

Contents lists available at ScienceDirect

ISA Transactions

journal homepage: www.elsevier.com/locate/isatrans

Research article

A coordinated MIMO control design for a power plant using improved sliding mode controller

Mohammad Ataei, Rahmat-Allah Hooshmand *, Siavash Golmohammadi Samani

Department of Electrical Engineering, Faculty of Engineering, University of Isfahan, Hezar-Jerib St., P. code: 8174673441, Isfahan, Iran

ARTICLE INFO

Article history:
Received 23 September 2012
Received in revised form
16 September 2013
Accepted 16 September 2013
Available online 7 October 2013
This paper was recommended for publication by Prof. Ahmad B. Rad.

Keywords:
Steam power plant
Boiler–turbine system
Sliding mode control
Throttle steam pressure

ABSTRACT

For the participation of the steam power plants in regulating the network frequency, boilers and turbines should be co-ordinately controlled in addition to the base load productions. Lack of coordinated control over boiler–turbine may lead to instability; oscillation in producing power and boiler parameters; reduction in the reliability of the unit; and inflicting thermodynamic tension on devices. This paper proposes a boiler–turbine coordinated multivariable control system based on improved sliding mode controller (ISMC). The system controls two main boiler–turbine parameters i.e., the turbine revolution and superheated steam pressure of the boiler output. For this purpose, a comprehensive model of the system including complete and exact description of the subsystems is extracted. The parameters of this model are determined according to our case study that is the 320 MW unit of Islam-Abad power plant in Isfahan/Iran. The ISMC method is simulated on the power plant and its performance is compared with the related real PI (proportional-integral) controllers which have been used in this unit. The simulation results show the capability of the proposed controller system in controlling local network frequency and superheated steam pressure in the presence of load variations and disturbances of boiler.

1. Introduction

Frequency control is one of the main factors for power network stability. For the participation of the steam power plants in regulating the network frequency, boilers and turbines should be controlled coordinately, so that the turbine can quickly respond to the power system load demand. Moreover, the boiler should be able to keep its parameters at the desired values whose most important state variable is the throttle steam pressure. The throttle pressure is the main output steam pressure of the boiler which enters the turbine. In order to achieve the control objectives, the system components including boiler, turbine, and the governor should be modelled and controlled precisely.

Today, most of the control systems of power plants are PI type controllers designed on the base of the linear strategies for single input–single output (SISO) systems [1–3]. However, the boiler–turbine is a nonlinear multi-input multi-output (MIMO) system with high coupling between state variables. Moreover, in many previous researches, the frequency control loop was not modelled and only the power (MW) control loop was considered [2,4,5]. It should be noted that there is actually frequency feedback as two inner–outer loops in addition to power (MW) control loop in turbine control system.

Various control systems have been designed for the boiler–turbine of the steam power plant so far, but they have their own advantages and disadvantages and can be divided into two main categories. The first group comprises intelligent approaches such as genetic algorithm (GA) and fuzzy logic [4,6], and neural networks [7]. These methods work on the basis of the input–output data and the physical subsystems are considered as black boxes. Therefore, their weakness is in the modelling of the internal dynamics. The second group comprises some classical approaches such as predictive control [1], linear quadratic Gaussian (LQG) [8], LQG/LTR (LQG with loop transfer recovery) [9], iterative feedback tuning (IFT) [10], H∞ control [11–13], and some combinations of these methods. Many of these methods are based on the linearized model of the system. Regarding the nonlinear behaviour of the power plant model and also wide range of operating conditions, the error due to linearization will be significant. Therefore, the control methods which deal with nonlinear model of the system and are robust against the disturbances and system uncertainties have attracted a great deal of attention [14,15]. Hence, variable structure controllers like sliding mode control (SMC) method can be used in this regard [8].

It should be noted that most of the studies have been accomplished on separate control of the boiler and turbine. Since some parameters of the boiler and turbine are highly coupled, therefore individual control of each parameter at the

* Corresponding author. Tel.: +98 311 7934073; fax: +98 311 7933071.
E-mail addresses: Ataei@eng.ui.ac.ir (M. Ataei), Hooshmand_r@eng.ui.ac.ir, Hooshmand_r@yahoo.com (R.A. Hooshmand), Samani25@gmail.com (S.G. Samani).

0019-0578/$ - see front matter © 2013 ISA. Published by Elsevier Ltd. All rights reserved.
http://dx.doi.org/10.1016/j.isatra.2013.09.015

expense of neglecting the coupling effects has no efficiency in unified control mode [16]. Therefore, coordinated control of the boiler and turbine is important and due to the interactions between these parts, they should be considered as two components of a unity system [8]. In other words, we encounter a multivariable control system.

In this paper, a proposed MIMO control system based on the SMC method for the coordinated control of the turbine revolution (frequency) and steam pressure of the boiler output in a steam power plant is designed. In this regard, complete and exact model of the subsystems including turbo-generator, turbine, and related control systems are used. In this comprehensive modelling, an effort has been made to consider all control loops and the signals related to the dispatching control of the boiler and turbine systems. Finally, the proposed method is simulated on Islam-Abad power plant in Isfahan/Iran and its performance is evaluated in the face of load changes and the boiler disturbances.

2. Modelling of the steam power plant

Modelling of the boiler–turbine system components is an important step before designing the related control system. Since, the design procedure is performed on the basis of Islam-Abad power plant (Isfahan/Iran), the corresponding models of subsystems are used. The model selection is done by considering the trade-off between the simplicity and completeness of the model to include the important dynamics of the turbine–boiler system. The general block diagram of the control system of the unit under study is shown in Fig. 1. In the following, different parts of this diagram are explained.

2.1. The boiler–turbine control system

In each unit of the steam power plant, the unit load demand signal is created by receiving the command signal from the area generation control (AGC) system and network frequency feedback, considering the capability of the unit. This fact has been shown as the MW Demand sub-block in Fig. 1. The created load demand signal enters into the boiler–turbine coordinated control system. This system, by getting feedback from the present actual MW of the unit and throttle steam pressure, creates the corresponding commands to the boiler and turbine in order to modify the amount of production. This means that the turbine–boiler control system not only acts on the bases of AGC command system but other factors including the main steam pressure, network frequency, and the boiler capability are also considered when making decision about changing the production. For instance, if load increasing demand is announced by the network and the main steam pressure is not desirable, the steam unit responds to this demand after the modification of the steam pressure.

The load demand signal affects both the boiler and the turbine simultaneously so that just after changing the governing status of the turbine valves, the boiler also changes its output. Moreover, if the control system functions properly in a coordinated relation, the turbine is so controlled that it provides the required load steam flow, while the boiler is controlled to provide the required steam flow of the turbine with the desired temperature and pressure.

The boiler–turbine coordinated control system has two coupled PI controllers. One of them is designed to control the unit production load in order to participate in the error correction of the network frequency. The other controller has the duty of controlling the throttle steam pressure which is the boiler output super-heated steam pressure entering the turbine. However, the performance of these controllers are not independent but interacted [17,18] and will be explained in Section 3.

In fact, the boiler–turbine coordinated control system includes two sub-systems. One is the turbine revolution control sub-system which is the same conventional loop of the turbine load–frequency control (LFC). The other is the control loop of the throttle steam pressure. This loop, by measuring the super-heated steam

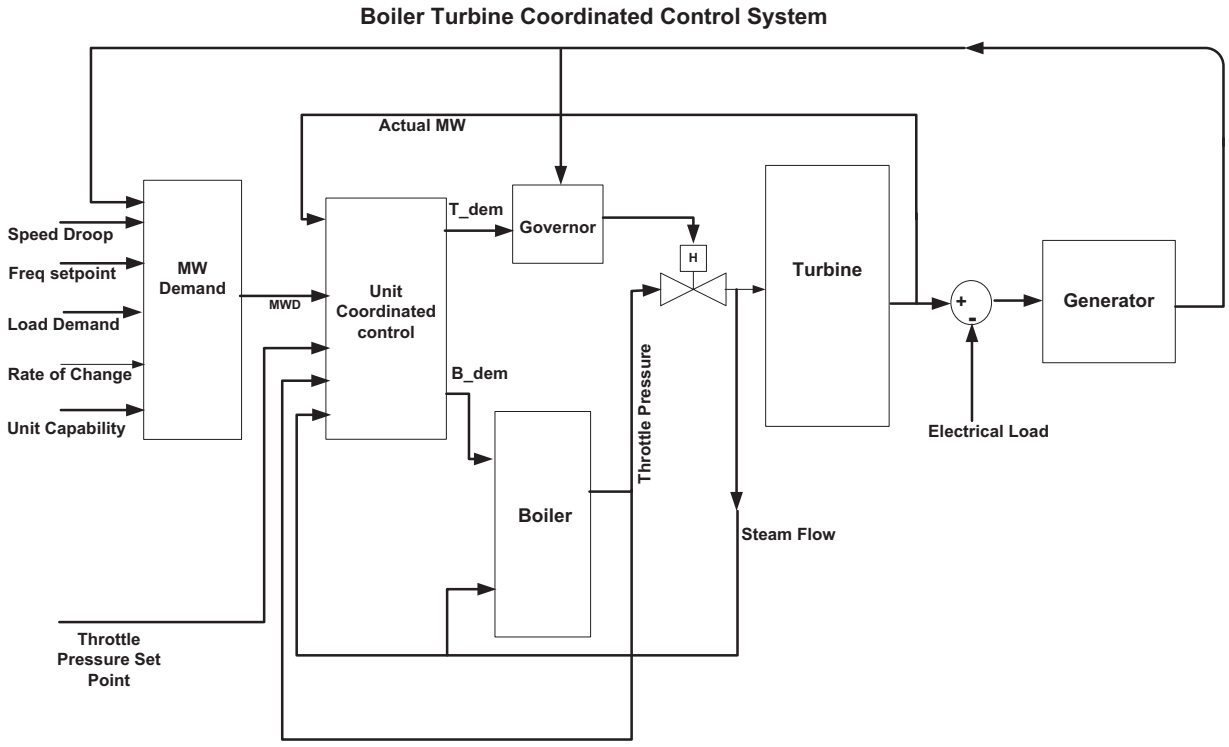

Fig. 1. The general control system block diagram of Islam-Abad power plant.

pressure and comparing it with a reference value, provides the corresponding commands for the fuel and air, and supplies water control sub-loops.

2.2. The state space description of the system

For applying the proposed control method, it is required to determine the state space equations of the system under study. For this purpose, based on the block diagram of Fig. 1, the state vector of the system containing 10 state variables is considered as follows:

$$X = (x_1, x_2, \ldots, x_{10}) = (D_Q, M_W, P_D, P_T, S_r, C_v, N_{hp}, N_{ip}, N_{lp}, dw) \quad (1)$$

In the following the state variables of the system are introduced as

D_Q	Thermal flow from furnace to water walls
M_w	Water flow in the water walls
P_D	Drum pressure
P_T	Throttle steam pressure
S_r	State variable related to the speed relay in the governor
C_v	Opening percentage of the governing valves
N_{hp}	Mechanical power of the high pressure turbine
N_{ip}	Mechanical power of the intermediate pressure turbine
N_{lp}	Mechanical power of the low pressure turbine
dw	Frequency difference

The inputs of the system are also as follow:

u_1	Control percentage of the boiler fuel valve
u_2	Control percentage of the turbine valve

2.2.1. The state equations of the boiler

The boiler model has been selected based on the Demello model [19,20] which is a common and parametric model. This model includes the dynamics of the boiler pressure and flow and is sufficient for our study. Based on this, the state equations of the drum boiler are described as follow:

$$\dot{x}_1 = -\frac{1}{T_{fu}}x_1 + \frac{1}{T_{fu}}u_1 \quad (2)$$

$$\dot{x}_2 = -\frac{1}{T_w}x_2 + \frac{1}{T_w}x_1 \quad (3)$$

$$\dot{x}_3 = \frac{1}{C_D}x_2 - \frac{K_b\sqrt{x_3 - x_4}}{C_D} \quad (4)$$

$$\dot{x}_4 = \frac{K_b\sqrt{x_3 - x_4}}{C_{SH}} - \frac{x_4 x_6}{C_{SH}} \quad (5)$$

where

T_{fu}	Combustion time constant
T_w	Water walls time constant
K_b	Pressure drop coefficient between drum and throttle
C_{SH}	Storing coefficient of super heated pipes
C_D	Storing coefficient of drum

2.2.2. The state equations of the governor

According to the related power plant unit, the model of the governor has been considered as a hydraulic-mechanical model including the control parameters of the corresponding unit [21]. The state equations of the governor are as follow:

$$\dot{x}_5 = -\frac{1}{T_{SR}}x_5 + \frac{1}{T_{SR}}\left(u_2 - x_4 x_6 - \frac{x_{10}}{R}\right) \quad (6)$$

$$\dot{x}_6 = -\frac{1}{T_{sm}}x_6 + \frac{1}{T_{sm}}x_5 \quad (7)$$

where,

T_{SR}	Speed relay time constant
T_{sm}	Servomechanism time constant
R	Speed droop

2.2.3. The state equations of the turbine

The turbine model has been considered based on the model of the power plant unit which is a three-stage model with reheat and the control parameters are also included. The state equations of the turbine are described as follow [21,23]:

$$\dot{x}_7 = -\frac{1}{T_{ch}}x_7 + \frac{F_{hp}}{T_{ch}}x_4 x_6 \quad (8)$$

$$\dot{x}_8 = -\frac{1}{T_{co}}x_8 + \frac{1}{T_{co}}\frac{F_{lp}}{F_{ip}}(x_9 - x_8 - x_7) \quad (9)$$

$$\dot{x}_9 = \frac{1}{T_{ch}}x_7 + \frac{F_{lp}}{T_{ch}}x_4 x_6 - \frac{1}{T_{rh}}(x_9 - x_8 - x_7) + \frac{1}{T_{rh}}\frac{F_{ip}}{F_{hp}}x_7 - \frac{1}{T_{co}}x_8 + \frac{1}{T_{co}}\frac{F_{lp}}{F_{ip}}(x_9 - x_8 - x_7) \quad (10)$$

where

T_{ch}	Steam chest time constant
T_{rh}	Reheat time constant
T_{co}	Cross over time constant
F_{hp}	Participation portion of the high pressure turbine in the produced mechanical power
F_{ip}	Participation portion of the intermediate pressure turbine in the produced mechanical power
F_{lp}	Participation portion of the low pressure turbine in the produced mechanical power

2.2.4. The state equations of the generator

The dynamic equation of the generator is as follows [21,23]:

$$\dot{x}_{10} = -\frac{D}{M}x_{10} + \frac{1}{M}x_9 - \frac{1}{M}d_l \quad (11)$$

where,

M	Generator inertial constant
D	Generator damping coefficient
d_l	Electric load disturbance

Since the boiler–turbine–generator system is a two-input two-output system with 10 state variables, the proposed SMC method should be improved in multi-input multi-output framework.

3. Control block diagram of the power plant

The complete block diagram of the boiler–turbine system is shown in Fig. 2. This figure shows the models of the boiler, turbine, governor, electric load in addition to the generator and boiler–turbine control system.

As mentioned before, the boiler–turbine control system used in the Islam-Abad power plant includes two coupled PI controllers. In other words, according to Fig. 2, the feedback paths for both PI controllers interacted with each other in a manner that the multivariable system could not be considered as a diagonal MIMO system including two separate SISO systems.

The system response to the load variations is slow with high overshoot and undershoots. Moreover, regarding the nonlinearity

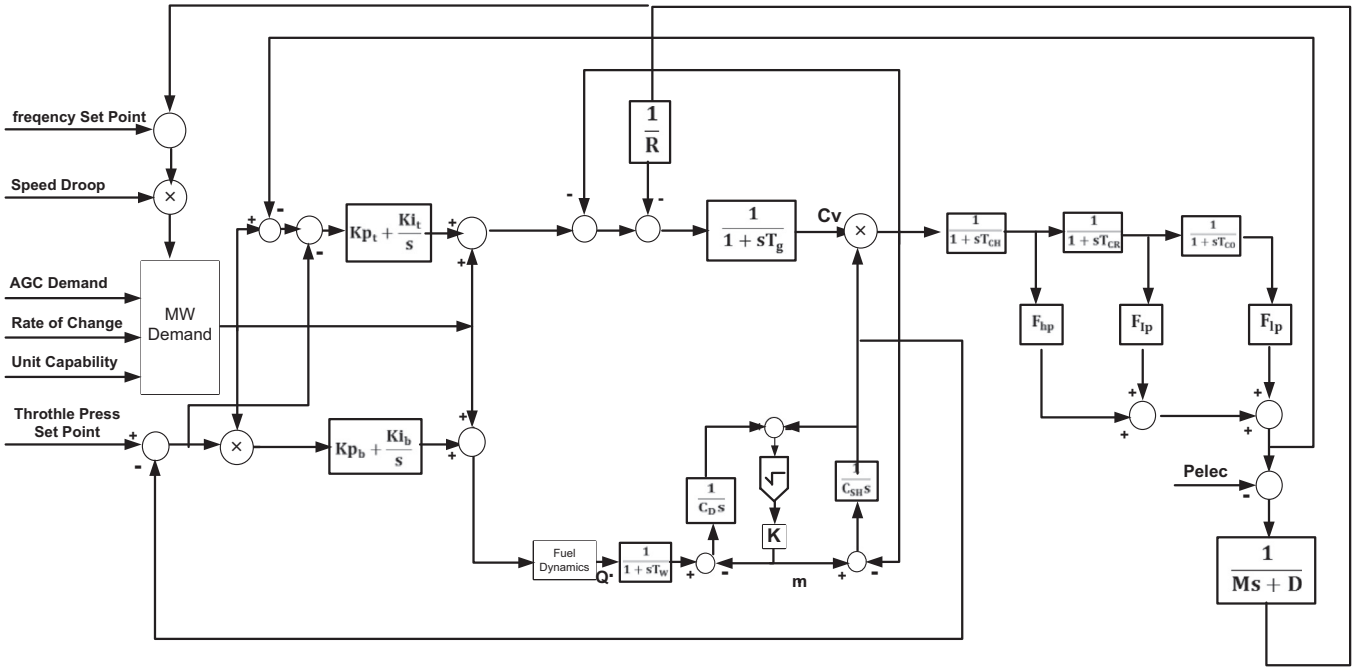

Fig. 2. The complete block diagram of the boiler–turbine system of Islam-Abad power plant.

of the boiler–turbine system, by changing the operational point and system parameters, the abilities of these controllers are degraded. In order to overcome these drawbacks, these controllers are substituted by an improved sliding mode controller, in the next section.

4. Design of the proposed controller

The sliding mode controller with different positive characteristics including the robustness against the parameter changes, external disturbances, and uncertainties; and quick dynamic response and simplicity of design is applicable in various nonlinear systems control [22]. For this purpose, the nonlinear system is considered in the following canonical dynamic equations:

$$x^{(n)} = f(x) + b(x)u + d(t) \tag{12}$$

In this equation, $f(x)$ and $b(x)$ are uncertain nonlinear functions with known uncertainty bounds whose bounds are denoted by $\widehat{f}$ and $\widehat{b}$. Furthermore, the $d(t)$ function is related to the disturbance entering the system.

In this equation, $\mathbf{x}(t) = [x(t)\ \dot{x}(t) \ldots x^{(n-1)}(t)]^T \in R^n$ is the system state vector. By assigning the desirable state vector $\mathbf{x}_d(t)$, the error state vector can be shown as follows:

$$\mathbf{E}(t) = \mathbf{x}(t) - \mathbf{x}_d(t) = [e(t)\ \dot{e}(t) \ldots e^{(n-1)}(t)]^T \tag{13}$$

The first step in designing the sliding mode controller is to define an appropriate sliding surface in the state space entitled as switching function considered as follows:

$$s = (D+\lambda_1)(D+\lambda_2)\ldots(D+\lambda_{(n-1)})e \quad D = \frac{d}{dt} \tag{14}$$

The second step is to determine the control law for conducting the system to the selected sliding surface. In this method, the control law always consists of two parts as shown in the following equation:

$$u(t) = u_{eq}(t) - u_n(t) \tag{15}$$

where,

$$u_{eq}(t) = \hat{b}^{-1}(x_r^{(n-1)} - \hat{f}) \tag{16}$$

$$x_r^{(n-1)} = x_d^{(n)} - b_1 x^{(n-1)} + b_1 x_d^{(n-1)} - \ldots - b_{n-1}\dot{x} + b_{n-1}\dot{x}_d \tag{17}$$

In the conventional SMC, $u_n(t)$ is considered as the sign function, however the controller can be improved by using other useful forms for $u_n(t)$. In the following, the proposed SMC is presented in a Lemma for SISO [22] and is extended for MIMO systems. It should be noted that the related controller is called ISMC in this paper.

Lemma. *Let the nonlinear system description be as relation (12). In order to achieve the convergence of the system states to a predetermined sliding surface, the control law is proposed as follows:*

$$u(t) = u_{eq}(t) - w \tag{18}$$

where,

$$w = \hat{b}^{-1}[(F + \alpha e^{-\frac{\beta}{|S|}})\tanh\left(\frac{S}{\varepsilon}\right) + \gamma S] \tag{19}$$

provided that $\alpha \succ \eta, \alpha - \eta \prec 2Fe^{\frac{-\beta}{|S|}}$

Proof. Before presenting the proof, some basic justifications about the method is explained. The function W is in the form of an exponential function whose plot versus switching function is shown in Fig. 3. As it is seen, for small values of S, the equivalent input becomes such that the system states are kept in a narrow boundary layer around the sliding surface. Moreover, whenever the distance from sliding surface becomes larger, the decay rate over a period of time is increased. This is performed through inserting larger input with an exponential rate. The important point is that the function W should be selected in a manner that the Lyapunov stability conditions are satisfied and it is guaranteed that S is converged to zero. This is proved in the following.

At first, the proof is presented for SISO system and then it is extended to multivariable case. In this way, the sliding surface is selected according to relation (14). So we have:

$$\dot{s} = f + bu - x_r^{(n)} \tag{20}$$

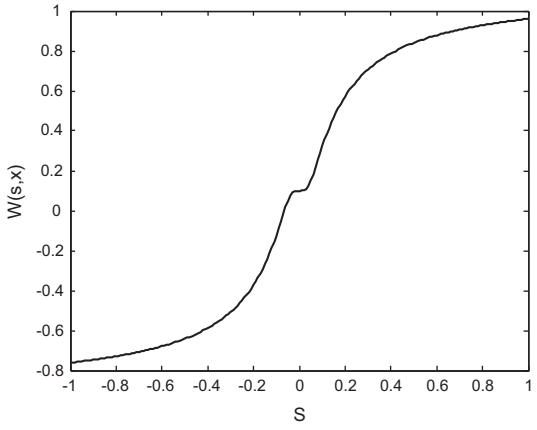

Fig. 3. The plot of W function versus switching function in ISMC method.

So, the Lyapunov candidate is considered as follows:

$$V=\frac{1}{2}S\cdot S^{T} \tag{21}$$

Also, the following sliding condition is considered:

$$S\dot{S}\le -\eta|s|e^{-\frac{\beta}{|s|}}-\gamma s^{2} \tag{22}$$

Regarding the previous relations and using the proposed control law, it can be written:

$$s(f+bu-x_r^{(n)})\le -\eta|s|e^{-\frac{\beta}{|s|}}-\gamma s^{2}\rightarrow s(f-\hat{f})+\eta|s|e^{-\frac{\beta}{|s|}}+\gamma s^{2}\le bws \tag{23}$$

In the case of $s\ge 0$ we have:

$$(f-\hat{f})+\eta e^{-\frac{\beta}{|s|}}+\gamma s\le bw \tag{24}$$

According to the above relation, by satisfying the condition of $\alpha>\eta$ in the lemma, w can be derived as follows:

$$w=\hat{b}^{-1}[(F+\alpha e^{-\frac{\beta}{|s|}})+\gamma s] \tag{25}$$

In the case of $s\le 0$ also we have:

$$(f-\hat{f})-\eta e^{-\frac{\beta}{|s|}}+\gamma s\ge bw \tag{26}$$

Considering the upper uncertainty bounds as $|\hat{f}-f|\le F$, in order to satisfy the relation (26), w can be selected as follows:

$$w=\hat{b}^{-1}[-(F+\alpha e^{-\frac{\beta}{|s|}})+\gamma s] \tag{27}$$

Combining Eqs. (25) and (27) for two cases, the following unified relation for w can be achieved:

$$w=\hat{b}^{-1}[(F+\alpha e^{-\frac{\beta}{|s|}})sign(s)+\gamma s] \tag{28}$$

In order to avoid chattering phenomenon, the function w is improved as follows:

$$w=\hat{b}^{-1}[(F+\alpha e^{-\frac{\beta}{|s|}})\tanh\left(\frac{S}{\varepsilon}\right)+\gamma s] \tag{29}$$

By using the above SMC, in addition to deleting the chattering, the dynamic behaviour of the system is controlled in a way that when the system trajectory is far from sliding surface, the control signal can guide the trajectory to the sliding surface with high speed of convergence. In continuation, the proof is extended for multi-input multi-output systems. For this purpose, a vector of sliding surfaces is considered as:

$$s=[s_1 s_2 ... s_n]^{T} \tag{30}$$

where,

$$s_i=(D+\lambda_{i1})(D+\lambda_{i2})...(D+\lambda_{i(n-1)})e_i,\quad D=\frac{d}{dt} \tag{31}$$

The function w which is used in the control law is in vector form as follows:

$$w=[w_1 w_2 ... w_n]^{T} \tag{32}$$

where,

$$w_i=[(F_i+\alpha_i e^{-\frac{\beta_i}{|s_i|}})\tanh\left(\frac{s_i}{\varepsilon_i}\right)+\gamma_i s_i],\quad i=1,2,3,..,n \tag{33}$$

In this case the related parameters should be selected accordingly so that the following sliding conditions are satisfied:

$$S_i\dot{S}_i\le -\eta_i|s_i|e^{-\frac{\beta_i}{|s_i|}}-\gamma_i {s_i}^{2},\quad i=1,2,3,..,n \tag{34}$$

Then, similar to the SISO case, the control law can be achieved as the following equation:

$$U=\hat{B}^{-1}({x_r}^{(n-1)}-\hat{f}-W) \tag{35}$$

5. Applying the proposed control method to the Islam-Abad power plant in Isfahan/Iran

Before explaining the design procedure of the proposed control method, it should be noted that in order to simplify the controller design, a reduced order model of the system is used. For this purpose, since the time constant of the two state variables of the governor is small, the governor is modelled by a state with a time constant equal to the sum of the related main ones. For the turbine also, since the time constant of the high pressure turbine is small and the reheat time constant is large, only the response of high pressure turbine is taken into consideration. Therefore, the simplified model of the boiler–turbine system with six states is achieved and states x_1 to x_6 replace states x_1, x_4, x_3, x_6, x_7 and x_{10} of the full order model, respectively. It should be noted that the simplified model is used only for the design of the controller and then the designed controller is implemented in the full order model. Apart from the above-mentioned point, the second point which should be considered in the design procedure of the proposed control law for the multivariable boiler–turbine system of the power plant is that the straightforward method of SMC will encounter a problem that the matrix B is not invertible. This is due to the nature of the dynamical equations in which only the input u_2 appears in the state equations related to the state variables x_2 and x_6, while u_1 does not appear explicitly. However, considering whatever happens in the real power plant, we should rewrite the equations so that input u_1 appears in the state equation of the variable x_2 and the input u_2 appears in the state equation of the variable x_6. In this case, state variables x_2 and x_6 are in fact controllable by inputs u_1 and u_2 respectively. It should be noted that, this problem is independent of the model order reduction mentioned in the beginning of the paragraph. For this purpose, the following mathematical manipulations are carried out:

$$C_{SH}\ddot{x}_2=x_1-C_D\ddot{x}_3-T_t\ddot{x}_5-\dot{x}_5 \tag{36}$$

$$M\dddot{x}_6=-D\ddot{x}_6+\ddot{x}_5-\ddot{d}_l \tag{37}$$

$$C_{SH}\ddot{x}_2=-\frac{1}{T_{fu}}x_1+\frac{1}{T_{fu}}u_1-C_D\ddot{x}_3-T_t\ddot{x}_5-\dot{x}_5 \tag{38}$$

$$\begin{aligned}M\dddot{x}_6&=-D\ddot{x}_6-\frac{1}{T_t}\dot{x}_5+\frac{1}{T_t}\dot{x}_2x_4+\frac{1}{T_t}x_2\dot{x}_4-\ddot{d}_l\\&=-D\ddot{x}_6-\frac{1}{T_t}\dot{x}_5+\frac{1}{T_t}\dot{x}_2x_4+\frac{1}{T_tT_g}x_2x_4+\frac{1}{T_tT_g}x_2u_2-\frac{1}{T_tT_gR}x_2x_6-\ddot{d}_l\end{aligned} \tag{39}$$

It should be noted that T_g is the time constant of the governor which is equal to $T_{sm}+T_{SR}$. As it is seen, in the equations related to variables x_2, and x_6, inputs u_1 and u_2 appears, respectively.

In continuation, the sliding surfaces are selected as follow:

$$s_1 = \dot{e}_1 + b_1 e_1 \tag{40}$$

$$s_2 = \ddot{e}_2 + c_1 \dot{e}_1 + c_2 e_2 \tag{41}$$

where e_1 and e_2 are the state errors and b_1, c_1, and c_2 are some design parameters. By differentiating and substituting, we have:

$$\dot{s}_1 = \ddot{x}_2 - \ddot{x}_{2d} + b_1 \dot{x}_2 - b_1 \dot{x}_{2d} \tag{42}$$

$$\dot{s}_1 = \frac{1}{C_{SH}}\left(-\frac{1}{T_b}x_1 + \frac{1}{T_b}u_1 - C_D \ddot{x}_3 - T_t \dddot{x}_5 - \ddot{x}_5\right) - \ddot{x}_{2d} + \frac{b_1}{C_{SH}}(x_1 - C_D \dot{x}_3 - T_t \ddot{x}_5 - x_5) - b_1 \dot{x}_{2d} \tag{43}$$

$$\dot{s}_2 = \dddot{x}_6 - \dddot{x}_{6d} + c_1 \ddot{x}_6 - c_1 \ddot{x}_{6d} + c_2 \dot{x}_6 - c_2 \dot{x}_{6d} \tag{44}$$

$$\dot{s}_2 = \frac{1}{M}\left(-D\ddot{x}_6 - \frac{1}{T_t}\dot{x}_5 + \frac{1}{T_t}\dot{x}_2 x_4 - \frac{1}{T_t T_g}x_2 x_4 + \frac{1}{T_t T_g}x_2 u_2 - \frac{1}{T_t T_g R}x_2 x_6 - \ddot{d}_l\right) - \dddot{x}_{6d} + c_1 \ddot{x}_6 - c_1 \ddot{x}_{6d} + c_2 \dot{x}_6 - c_2 \dot{x}_{6d} \tag{45}$$

In order to use Eq. (35) for computing the control signal, at first, $\hat{B}^{-1}$ can be calculated as follows:

$$\hat{B}^{-1} = \begin{bmatrix} \frac{1}{T_{fu}C_{SH}} & 0 \\ 0 & \frac{x_2}{MT_{ch}T_g} \end{bmatrix}^{-1} = \begin{bmatrix} T_{fu}C_{SH} & 0 \\ 0 & \frac{MT_{ch}T_g}{x_2} \end{bmatrix} \tag{46}$$

Then, the control laws u_1 and u_2 are achieved

$$\begin{bmatrix} u_1 \\ u_2 \end{bmatrix} = -\begin{bmatrix} T_{fu}C_{SH} & 0 \\ 0 & \frac{MT_{ch}T_g}{x_2} \end{bmatrix} \times \left\{ \begin{bmatrix} G_1 \\ G_2 \end{bmatrix} + \begin{bmatrix} k_1 \mathrm{sgn}(s_1) \\ k_2 \mathrm{sgn}(s_2) \end{bmatrix} \right\} \tag{47}$$

where G_1 and G_2 are as follow:

$$G_1 = \frac{1}{C_{SH}T_b}x_1 - \frac{C_D}{C_{SH}}\ddot{x}_3 - \frac{1}{C_{SH}}(T_t \dddot{x}_5 - \ddot{x}_5) - \ddot{x}_{2d} + \frac{b_1}{C_{SH}}(x_1 - C_D \dot{x}_3 - T_t \ddot{x}_5 - x_5) - b_1 \dot{x}_{2d} \tag{48}$$

$$G_2 = \frac{1}{M}\left(-D\ddot{x}_6 - \frac{1}{T_t}\dot{x}_5 + \frac{1}{T_t}\dot{x}_2 x_4 - \frac{1}{T_t T_g}x_2 x_4 - \frac{1}{T_t T_g R}x_2 x_6\right) - \ddot{d}_l - \dddot{x}_{6d} + c_1 \ddot{x}_6 - c_1 \ddot{x}_{6d} + c_2 \dot{x}_6 - c_2 \dot{x}_{6d} \tag{49}$$

It should be noted that for the simulation of the proposed method, according to Eqs. (33) and (35), the sign functions are replaced by suitable functions using the presented lemma where the control laws of u_1 and u_2 presented in Eq. (47) can be improved as follows:

$$\begin{bmatrix} u_1 \\ u_2 \end{bmatrix} = -\begin{bmatrix} T_{fu}C_{SH} & 0 \\ 0 & \frac{MT_{ch}T_g}{x_2} \end{bmatrix} \times \left\{ \begin{bmatrix} G_1 \\ G_2 \end{bmatrix} + \begin{bmatrix} (F_1 + \alpha_1 e^{-\frac{\beta 1}{|s1|}})\tanh\left(\frac{s_1}{\varepsilon_1}\right) + \gamma_1 s_1 \\ (F_2 + \alpha_2 e^{-\frac{\beta 2}{|s2|}})\tanh\left(\frac{s_2}{\varepsilon_2}\right) + \gamma_2 s_2 \end{bmatrix} \right\} \tag{50}$$

In order to summarize the design procedure of ISMC, the step by step algorithm is explained as follows:

1. Based on the well-known common model of the steam power plant, special block diagram for the case study is derived as in Fig. 2.
2. The state space equations governing each sub-blocks including different main parts of the power plant such as boiler, governor, turbine, and generator are described. The relations are provided by Eqs. (2)–(11).
3. The required parameters for the state equations should be determined.
4. According to the design procedure presented in this section, the ISMC based control laws u_1 and u_2 should be determined using Eq. (50).
5. Implementing the obtained control inputs and evaluating the performance of the ISMC controller.

6. Simulation results

In this section, the simulation results of applying the proposed control system to the 320 MW unit of Islam-Abad power plant in Isfahan/Iran are evaluated and their performance is compared with the related real PI controllers which have been used in this unit. The model of this power plant is based on the block diagram in Fig. 2 whose related parameters are presented in the Appendix A.

6.1. The system response in case of using PI controller

First, it is assumed that only PI controller (PIC) has been used in the frequency control of the power plant. The step response of the state $\Delta\omega(t)$ to 0.1 pu load change is shown in Fig. 4a as a solid-line curve. As it is seen, the settling time is about 350 s and the overshoot of the step response is 0.006 pu (per unit) rad/s or 0.046 Hz. Therefore, the system response in the settling time and overshoot points of view is not acceptable and a more suitable controller is required. Moreover, the graph of the throttle steam pressure has been shown as a solid-line curve in Fig. 4b.

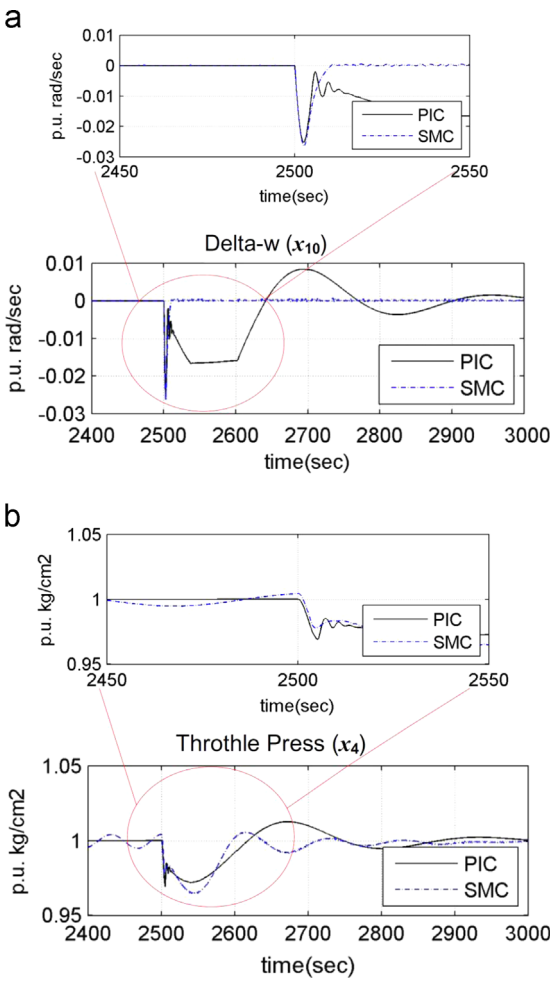

Fig. 4. The graph of the responses in the cases of using PI controller (with experimental parameters) and conventional SMC (with simulation parameters) in the face of 0.1 pu load change, (a) state $\Delta\omega(t)$, (b) throttle steam pressure.

6.2. The system response in case of using conventional SMC

Since the PIC performance of the previous subsection is not well acceptable, a nonlinear controller is investigated in this part. For this purpose, first a conventional SMC is designed and simulation results are examined. The step response of the state $\Delta\omega(t)$ to 0.1 pu load change and also graph of the throttle steam pressure are shown in Fig. 4. In this regard, it should be explained that by tuning the coefficients of controller and sliding surface, the response can be almost changed. For instance, by decreasing the sliding surface coefficient b_1, the oscillations can be eliminated; however, it makes the response speed slower as in Fig. 4. In this case, the rise and settling time are increased significantly. On the other hand, by increasing this coefficient, though the response speed is increased, it is oscillating. In this case, the response encounters chattering which is not desirable. On the other hand, chattering may excite the high frequency un-modelled dynamics of the system which can even lead to instability.

6.3. The improved SMC (ISMC)

In this subsection, the simulation results of applying the proposed controller to the power plant under study are presented and the performance of the controller is evaluated. The system behaviour in the face of step disturbance of 0.1 pu load change is shown in Figs. 5 and 6 for two cases of using PI controller and ISMC.

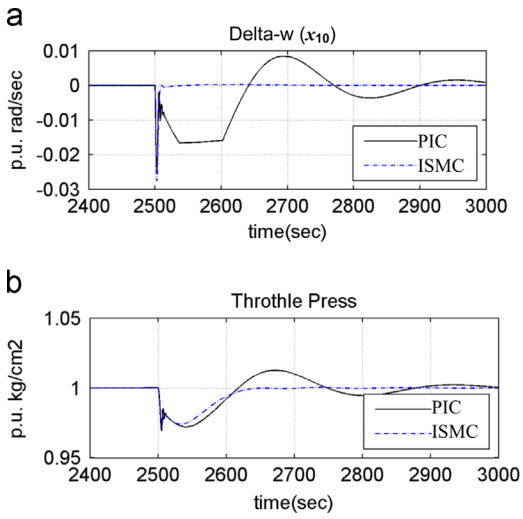

Fig. 5. Comparison of two control systems (PI controller with experimental parameters, and ISMC with simulation parameters) in the face of 0.1 pu load change, (a) frequency difference $\Delta\omega(t)$, (b) the throttle steam pressure,

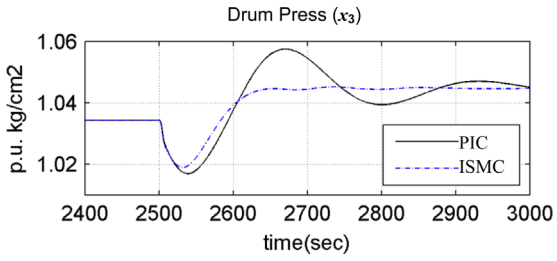

Fig. 6. Comparison of drum pressure response for two control systems (PI controller with experimental parameters, and ISMC with simulation parameters) in the face of 0.1 pu load change.

By comparing the simulation results, the following points are concluded.

(1) One of the positive features of the SMC is its fast transient state dynamics. This advantage is revealed in the results of the frequency control, i.e. the SMC has faster dynamics than that of the PIC. It should be noted that the simulations are performed regarding the practical considerations such as the limitations in the rate of changes rate in the fuel, air and steam inputs.
(2) In the case of using ISMC, the overshoot does not appear in the response of the throttle steam pressure. Moreover, the amount of throttle pressure drop is a little better than that in the case of using PI controller.
(3) From the chattering point of view, by comparing Fig. 5 with the magnified section of Fig. 4, one can observe the improvement of the ISMC method compared with the SMC.
(4) Although the dynamics of the drum pressure is not the objective of the control system, it affects the drum level dynamics. The change in drum pressure perturbs the drum

Table 1
Comparison of the responses specifications in the cases PIC, SMC and ISMC methods in the face of 0.1 pu load change.

	Method	Max. overshoot (%)	Rise time (s)
$\Delta\omega(t)$ or x_{10}	PIC	0.8	140
	SMC	0	10
	ISMC	0	10
Throttle pressure (x_4)	PIC	1.5	123
	SMC	0.5	73
	ISMC	0	245

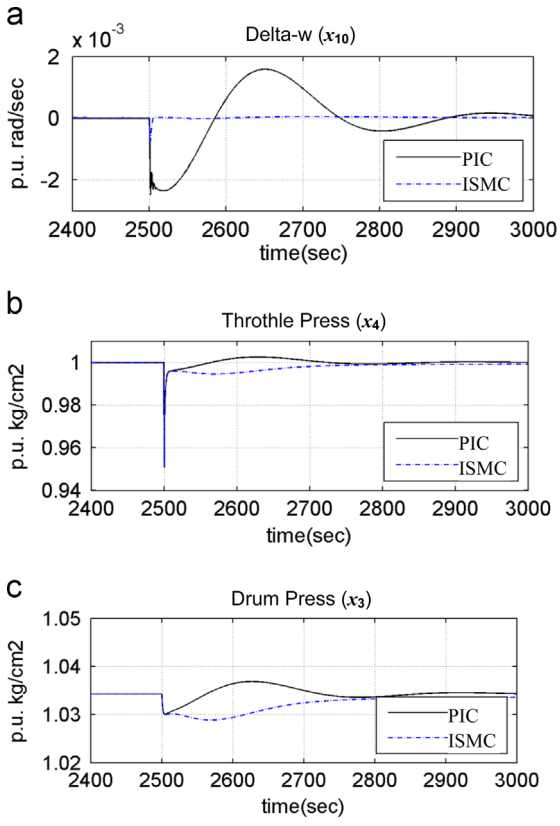

Fig. 7. Comparison of two control systems (PI controller with experimental parameters, and ISMC with simulation parameters) in the face of the pulse disturbance of 5% pressure drop in the throttle steam, (a) frequency difference $\Delta\omega(t)$, (b) throttle steam pressure, (c) drum pressure.

Table A.1
Parameters of the under study Islam-Abad power plant.

	Parameters	Values
Boiler and Turbo-generator	Boiler	$T_w=7$ s, $T_{fu}=5$ s $C_d=108$ s, $C_{sh}=12$ s $K_b=3.78$ s
	Turbine and governor	$T_{ch}=0.4$ s, $T_{rh}=7.65$ s $T_{co}=0.63$ s, $R=0.05$ $T_g=0.2$ s $0<u_1\leq 1$, $\lvert\dot{u}_1\rvert\leq 0.007$ $0<u_2\leq 1$, $-0.1<\dot{u}_1\leq 0.1$ $F_{hp}=0.29$, $F_{ip}=0.29$, $F_{lp}=0.42$
	Generator	$M=6$ s, $D=0.01$
The control systems	PI controller	$K_{pt}=1.08$, $K_{it}=3.24$, $K_{pb}=4.4$, $K_{ib}=0.04$
	Conventional SMC	$b_1=0.01$, $c_1=5$, $c_2=15$, $K_{smc1}=0.03$, $K_{smc2}=0.018$
	ISMC	$\alpha_1=2.9$, $\beta_1=0.005$, $\gamma_1=0.008$, $\varepsilon_1=0.5$, $F_1=0.05$ $\alpha_2=0.5$, $\beta_2=0.003$, $\gamma_2=0.004$, $\varepsilon_2=0.5$, $F_2=0.05$

level so that decreasing the drum pressure causes the increment of drum level and vice versa. The drum level is controlled in a limited bound and if it exceeds, the boiler keeper equipment starts operating and turning off the steam unit. Therefore, it is required that the drum level changes be gradual in system dynamics leading to more stability. From this point of view also, the SMC enjoys superiority.

In order to compare the specifications of the responses in the cases of PIC, SMC and ISMC methods, the maximum overshoot and rise time of the responses are summarized in Table 1.

The other disturbance which is imposed on the boiler–turbine system is the drop of the throttle steam pressure. This disturbance is due to some causes including trip in one or two couples of the boiler fire, increment of the circular gas flow of the boiler for controlling the reheat temperature, and a hole punched in the super-heater pipes, dropping the gas fuel pressure. In order to model these disturbances, a negative pulse or step should be applied to the throttle steam pressure in the boiler model.

The performance of the proposed control system is compared with classical one in response to the pulse disturbance of 5% pressure drop in the throttle steam as Fig. 7. As it is observed, the ISMC system has less overshoot and undershoots in controlling the frequency. The settling time of the response is also significantly less than the corresponding PI controller.

Regarding these figures, it is seen that the transient state dynamics of the system is significantly better than the corresponding control system with PI controller.

7. Conclusions

In this paper, the proposed SMC system was instituted instead of PI controllers for the coordinated control of the turbine revolution and steam pressure of the boiler output in Islam-Abad power plant in Isfahan/Iran. For this purpose, precise model of the subsystems including boiler, turbine, governor, and the related control systems were used. The simulation results show that the ISMC in controlling the frequency and throttle steam pressure enjoys greatly faster dynamic with respect to PI type controller, while all limitations on input changes of fuel, air, and steam are considered in the simulations. Moreover, there is no overshoot and undershoot in the system response. Also, the drum pressure dynamic which has a direct effect on the drum level dynamic is more desirable when using the SMC compared with PI controller.

Appendix A

The values of the parameters in block diagram of Fig. 2 related to Islam-Abad power plant are presented in Table A.1. It should be noted that the PI parameters are specified roughly based on catalogues and repertories available in the power plant and are finely tuned by expert engineers, as trial and error method after overhauling [23].

References

[1] Salehi M, Afzalian A. Robust H∞ control design for a boiler–turbine unit. In: 2008 international conference on smart manufacturing application; 2011. p. 520–5.
[2] Kim WG, Moon UC, Lee SC, Lee KY. Application of dynamic matrix control to a boiler–turbine system. In: 2005 IEEE conference on control application; 2005, vol. 2. p. 1595–1600.
[3] Takagi DMY, Mitsumoto K, Oguchi H, Nakai A, Hino S. A new control strategy for coal fired thermal power plants. In: 2005 IEEE conference on control applications; 2005. p. 1680–5.
[4] Wang Y, Yu X. New coordinated control design for thermal power generation units. IEEE Transactions on Industrial Electronics 2010;53:123–30.
[5] Yang S, Qian C, Du H. A genuine nonlinear approach for controller design of a boiler–turbine system. ISA Transactions 2012;51:446–53.
[6] Li Y, Shen J, Lee KY, Liu X. Offset-free fuzzy model predictive control of a boiler–turbine system based on genetic algorithm. Simulation Modeling Practice and Theory 2012;26:77–95.
[7] Zhang J, Zhang F, Ren M, Hou G, Fang F. Cascade control of superheated steam temperature with neuro-PID controller. ISA Transactions 2012;51:778–85.
[8] Kim WG, Moon UC, Lee SC, Lee KY. Fuzzy-adapted recursive sliding-mode controller design for nuclear power plant control. IEEE Transactions on Nuclear Science 2004;51:256–66.
[9] Liu XJ, Guan P, Liu JZ. Power plant coordinated predictive control using neuro fuzzy model. In: 2006 proceedings of the 2006 American control conference; 2006, vol. 1. p. 129–33.
[10] Zhang S, Taft CW, Bentsman J, Hussey A, Petrus B. Simultaneous gains tuning in boiler/turbine PID-based controller clusters using iterative feedback tuning methodology. ISA Transactions 2012;51:609–21.
[11] Wu J, Nguang SK, Shen J, Liu G, Li YG. Robust H∞ tracking control of boiler_turbine systems. ISA Transactions 2010;49:369–75.
[12] Abdennour AB, Lee KY. A decentralized controller design for a power plant using robust local controllers and functional mapping. IEEE Transactions on Energy Conversion 1996;11:394–400.
[13] Moradi H, Bakhtiari-Nejad F, Saffar-Avval M. Robust control of an industrial boiler system; a comparison between two approaches: sliding mode control & H∞ technique. Energy Conversion and Management 2009;50:1401–10.
[14] Tan W, Marquez HJ, Chen T. Multivariable Robust Controller Design for a Boiler System. IEEE Transactions on Control Systems Technology 2002;10:735–42.
[15] Peng H, Ozaki T, Ozaki VH, Toyoda Y. A Nonlinear Exponential ARX model-based multivariable generalized predictive control strategy for thermal power plants. IEEE Transactions on Control System Technology 2002;10:256–62.
[16] Shayeghi H, Shayanfar HA, Jalili A. Load frequency control strategies: a state-of-the-art survey for the researcher. Energy Conversion and Management 2009;50:344–53.
[17] Labibi B, Marquez HJ, Chen T. Decentralized robust PI controller design for an industrial boiler. Journal of Process Control 2009;19:216–30.
[18] Kunitomi K, Kurita A, Tada Y, Ihara S, Price WW, Richardson LM, et al. Modeling combined-cycle power plant for simulation of frequency excursions. IEEE Transactions on Power System 2003;18:724–9.
[19] Hu Z, Fan H, He Y. Robust controller design for boiler system, 2008. In: international conference on intelligent computation technology and automation; 2008. p. 445–9.
[20] de Mello FP, Fellow. Boiler models for system dynamic performance studies. IEEE Transactions on Power Systems 1991;6:66–74.
[21] IEEE Working Group on Prime Mover and Energy Supply Models for System Dynamic Performance Studies. Dynamic models for fossil fueled steam units in power system studies. IEEE Transactions on Power Systems 1991;6:753–61.
[22] Falahpoor M, Ataei M, Kiyoumarsi A. A chattering-free sliding mode control design for uncertain chaotic systems. Chaos, Solitons and Fractals 2009;42:1755–65.
[23] Italian GIE Catalogue, Design Catalogue of the Unit 5 in Islam-Abad Power Plant. Islam-Abad Power Plant, Isfahan, Iran.